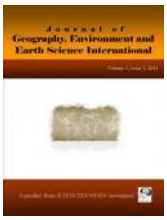

Journal of Geography, Environment and Earth Science International
6(1): 1-24, 2016; Article no.JGEESI.24388
ISSN: 2454-7352

SCIENCEDOMAIN *international*
www.sciencedomain.org

Natural Hazard Assessment and Monitoring in the Black Hills and Adjacent Areas, South Dakota and Wyoming, USA, Using Remote Sensing and GIS-Methods

Barbara Theilen-Willige[1*]

[1]*Institute of Applied Geosciences, Technische Universität Berlin (TUB), Ernst Reuter-Platz 1,10587 Berlin, Germany.*

Author's contribution

The sole author designed, analyzed, interpreted and prepared the manuscript.

Article Information

DOI: 10.9734/JGEESI/2016/24388
Editor(s):
(1) Wen-Cheng Liu, Department of Civil and Disaster Prevention Engineering, National United University, Taiwan and Taiwan Typhoon and Flood Research Institute, National United University, Taipei, Taiwan.
(2) Maria Manuela Portela, Department of Civil Engineering, Architecture and Georesources (DECivil), Instituto Superior Técnico, IST, Lisbon University, Portugal.
Reviewers:
(1) Ahmet Sayar, Kocaeli University, Turkey.
(2) Anonymous, Rochester Institute of Techno, USA.
(3) Helmi Zulhaidi Mohd Shafri, Universiti Putra Malaysia, Malaysia.
(4) Işin Onur, Akdeniz University, Turkey.
(5) Islam Abou El-Magd, National Authority for Remote Sensing and Space Sciences, Egypt.
(6) V. Sivakumar, Spatial Sciences and Disaster Management Group, C-DAC, Pune, India.
(7) Szu-Hsien Peng, Chienkuo Technology University, Taiwan.
Complete Peer review History: http://sciencedomain.org/review-history/14394

Original Research Article

Received 18th January 2016
Accepted 19th April 2016
Published 29th April 2016

ABSTRACT

This research considers the support provided by remote sensing and GIS methods for the delineation of potential sites susceptible to natural hazards such as earthquakes, flash floods and karst phenomena in the Black Hills area in South Dakota and Wyoming, USA.
By an integration of satellite data (Landsat, Sentinel), evaluations of digital elevation model data (DEM) and DEM derived morphometric maps, meteorological, geophysical and geological data in a GIS database an overview of potentially affected sites could be achieved. The analysis of digital enhanced satellite imageries, digital topographic data and open source geodata contributed to the acquisition of the specific tectonic, geomorphologic / topographic settings influencing local site

**Corresponding author: E-mail: Barbara.Theilen-Willige@t-online.de;*

conditions in the Black Hills area influencing the disposition to geo-hazards.
Weighed overlay tools in ArcGIS software helped to identify causal morphometric factors (such as flattest and lowest areas) influencing the susceptibility to flooding in case of flash floods. This tool was used as well to delineate areas susceptible to relatively higher earthquake ground motion due to local site conditions. Visual lineament analysis based on Landsat 8 and Sentinel radar images contributed to the detection of the tectonic / structural pattern influencing the development of karst phenomena (dolines/sinkholes). Dolines were mapped based on Landsat 8 and BingMap Aerial images.
Whenever a natural hazard occurs in the Black Hills and surrounding areas it can derived by the analysis of the above mentioned data and derived maps, which areas are likely to be more affected than others during future events.

Keywords: Black hills; South Dakota; remote sensing; GIS; natural hazards.

1. INTRODUCTION

Natural disasters have a considerable effect in human, infrastructure and economy. When natural hazards happen and affect cities and settlements such as in the area of the Black Hills, immediate and efficient actions are required which ensure the minimization of the damage and loss of human lives. Responding local and national authorities should be provided in advance with information where the highest damages due to local site conditions can be expected. The Black Hills situated within the states of Wyoming and South Dakota are prone to natural hazards as mentioned below [1,2,3]:

- Floods / Flash Floods
- Tornadoes
- Winter Storms
- Earthquakes
- Wildfires
- Karst, Dolines, Sinkholes
- Soil Erosion
- Droughts

Floods are among the most serious, devastating and costly natural hazards that affect the investigation area. The major drainage creeks of Alkali, Battle, Bear Butte, Beaver, Box Elder, Elk, French, Rapid, Spearfish, Spring, and Whitewood are all capable of causing heavy flooding and flood related damage [2].

There is a need to improve the inventory of areas that are more vulnerable to geo-hazards such as earthquake ground motions or to earthquake related secondary effects (landslides, liquefaction, soil amplifications), to flash floods, and to karst phenomena [4].

Satellite data provide reliable and rapid observation tools, supporting efforts for the mitigation of the impact of natural hazards and emergency response. The use of remote sensing and Geographic Information Systems (GIS) methods along with the related geo-databases assist local and national authorities to be better prepared and organized by taking into consideration the necessary information. The ability to undertake assessment, and monitoring can be improved to a considerable extent through the current advances in remote sensing and GIS technology. This is demonstrated by the example of earthquakes, flash floods and karst phenomena in the area of the Black Hills.

1.1 Objectives

The aim of this contribution was to develop adaptation strategies by presenting an approach in which Geographic Information Systems (GIS), used together with remote sensing data, contribute to the analysis and presentation of information, especially required for the different geo-hazards in the investigation area.

Causal or critical environmental factors influencing the disposition of settlements, industrial and infrastructural facilities to be affected by natural hazards and the potential damage intensity were analyzed interactively in a GIS database. The goal was to visualize the interactions and dependencies between causal / preparatory factors leading to local differences of the susceptibility to natural hazards.

One aspect was the analysis of the structural-tectonic pattern in the Black Hills area to detect fault and fracture zones that might affect or seismic wave propagation in case of stronger earthquakes. The investigation of the Landsat 8-data and Sentinel radar data for the detection of surface near fault and fracture zones and the structural pattern via visual lineament analysis was one of the main goals of this study.

Especially the Sentinel satellite radar images available since 2015 from ESA are assumed to trace sub-surface structures, partly not yet known in this detail, due to the radar backscatter of the surface enhancing subtle details of the morphology. Landsat 8 data available since 2013 show improvements as well in comparison with previous Landsat missions due to their more detailed radiometric resolution including thermal bands. Thus, one goal of this research was to investigate whether these newly available satellite data offer additional structural / tectonic information.

Further on, this research aims to study karst phenomena in the Black Hills area using remote sensing and GIS technologies as far as possible, in order to contribute to an inventory of karst features (dolines) and to the detection to some of the causal and triggering factors influencing their development and karstification processes. The more the knowledge of the structural setting in the subsurface (faults, fracture zones) influencing the development of karst processes can be improved, the better the infrastructure such as roads, bridges and buildings intersecting these karst phenomena can be planned or maintained.

1.2 Geographic and Geologic Setting

The Black Hills in western South Dakota and eastern Wyoming rise above the surrounding Great Plains. The Black Hills present a startling contrast to the surrounding topography. Its eastern side rises from the prairie (650 – 900 m height level) to a height from up to 2100 min the western part of the Black Hills (Fig. 1). The 290-km-long Black Hills uplift extends from the South Dakota-Nebraska border to southeast Montana. The general shape of the Black Hills is elliptical with a NNW-SSE-oriented axis.

The semi-arid climate conditions in the study area are characterized by cold winters and warm to hot summers. This combination of hot summers and limited precipitation in a semi- arid geography places South Dakota in a potential position of suffering a drought in any given year. On average, June is the wettest month of the year for the entire study area, with an average of18 percent of annual precipitation occurring. About one-third of average annual precipitation occurs during May and June enhancing the risk of flash floods during extreme events. November through February are consistently the driest

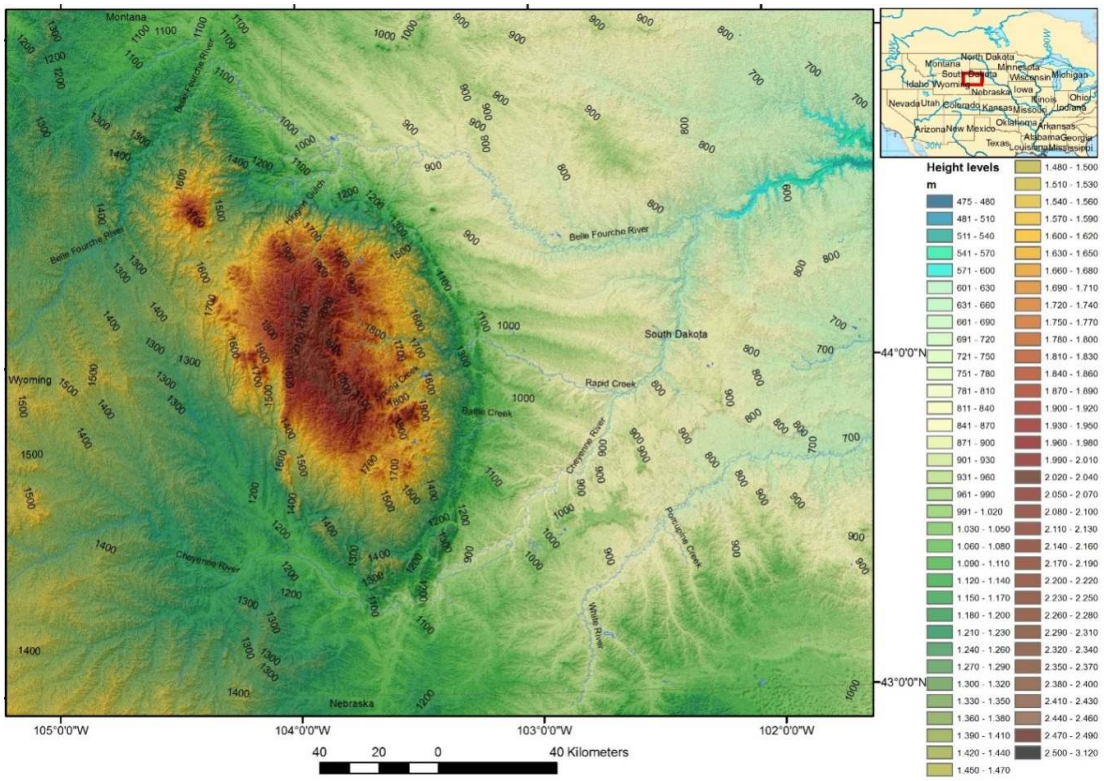

Fig. 1. Height level map based on ASTER GDEM data

months, with an average of 12.4 percent of annual precipitation occurring for the study area [5]. Fig. 2 provides an overview of the yearly precipitations [6].

The geologic situation in the investigation area has been studied intensely during the last centuries, at least due to the mineral resources found in this region [7,8,9].

Mainly three classes of rocks occur in this area: metamorphic, sedimentary, and igneous. The metamorphic rocks, schists, conglomerates, quartzites, and limestones, are exposed in the central part of the region. The sedimentary series, extending from Cambrian to Quaternary, consist of limestones, sandstones, and shales. The Black Hills uplift affected of two north-trending structural blocks, the mutual boundary of which marks a zone of recurrent movement, at least in the Phanerozoic. A Proterozoic core is exposed in the eastern block. A 20 Ma episode of alkalic magmatism associated with the Laramide orogenic event which started in the Late Cretaceous, 70 to 80 million years ago, and ended 35 to 55 million years ago, formed dikes, sills, stocks, laccolithic domes, diatremes and ring complexes. Composite intrusions formed laccolithic clusters doming the basement. These occur in a westerly trending band which crosses the uplift, possibly along a deep basement fault which offsets the boundary of the Archean and Proterozoic provinces [7,8,9].

Draping of the sedimentary section over basement fault blocks produced monoclines with, opposed to, and parallel to regional dip and ramps, terraces, and anticlines as subsidiary structures. The dominant fold trend is northward, although one major segment of the Black Hills monocline trends northwest. The folds terminate at intersections with other monoclines, by decreasing stratigraphic offset along strike, or by splaying into several folds of lesser structural relief [8]. Oligocene strata of the White River Group covered most of the eroded roots of the uplift as well as the basin. Epirogenic uplift in the Oligocene, and probably in the Miocene, and Pliocene, resulted in removal of most of these strata [8,9,10].

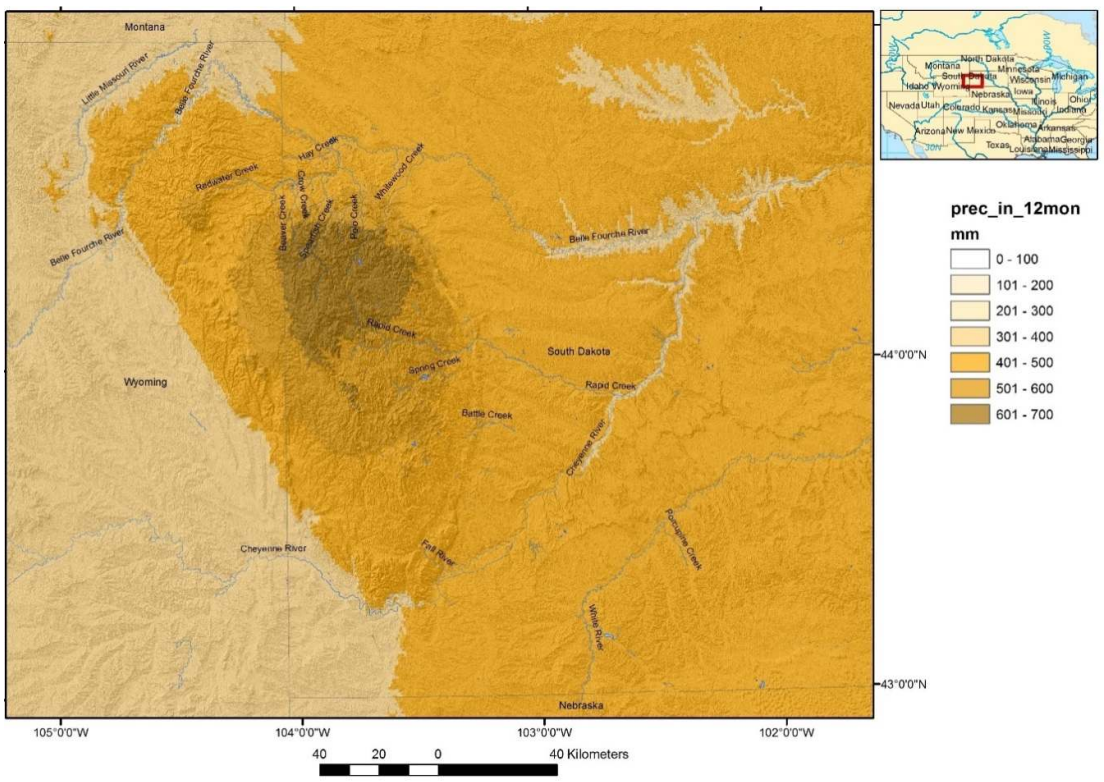

Fig. 2. Yearly precipitation according to WorldClim.org [6]

The data layers were generated through interpolation of average monthly climate data from weather stations on a 30 arc-second resolution grid (often referred to as "1 km2" resolution)

2. MATERIALS AND METHODS

GIS integrated remote sensing data and geospatial geodata analysis was used to visualize factors influencing the intensity of geo-hazards due to local site conditions. For example: the occurrence of higher earthquake shock and earthquake induced secondary effects is related to factors such as lithology (loose, unconsolidated sedimentary covers), higher groundwater tables and faults zones.

2.1 Evaluations of Landsat-data

Landsat data provided free by the USGS, EarthExplorer and the Global Land Cover Facility (GLCF), University of Maryland, USA were used for evaluations. The Landsat data were digitally processed using image processing and GIS software. Based on Landsat satellite data different false color composites (Red, Green, Blue - RGB combinations) of the different bands were used. The chosen image processing and RGB-combinations were focused on the enhancement of geologic, tectonic information. Low pass and high pass filters and directional variations supported the detection of subtle surface structures such as linear escarpments. Merging the "morphologic" image products derived from "Morphologic Convolution" image processing in ENVI software with RGB imageries, the evaluation feasibilities were improved. Unsupervised and supervised image classifications served as base for land use/cover mapping such as forests, wetlands, fields. Principal Component analysis (PC) of the Landsat 8-RGB images revealed structural and lithologic information as well. The oldest Landsat Multispectral Scanner (MSS) images taken between 1973 and 1979 play an important role as well. Due to less settlement and land use density at that time geologic information become partly better visible in spite of the lower spatial resolution (60 m).

Special attention was directed at precise mapping of traces of the tectonic pattern visible on satellite imageries, predominantly on areas with distinct expressed linear features (tonal linear anomalies, geomorphologic linear features, etc.). The combined evaluation of structural field data, seismotectonic data and lineament analysis based on remote sensing data has been carried out for decades in the Black Hills area [11,12,13], mainly based on Landsat 5 and ETM data and aerial images. Since the availability of Landsat 8-data the evaluation feasibilities have improved considerably due to the additional thermal bands.

As the methodology of lineament analysis is a very important component of this research, a short introduction into the background information seems to be useful for those readers who are not familiar with this methodology. The term lineament is a neutral term for all linear, rectilinear or slightly bended image elements. Lineaments are often expressed as scarps, linear valleys, narrow depressions, linear zones of abundant watering, drainage network, peculiar vegetation, landscape and geologic anomalies. Linear arrangement of pixels depicting the same color / gray tone were mapped as linear features, lineations or lineaments. Special attention was focused on precise mapping of traces of faults (linear anomalies in the drainage pattern, in the morphology or within outcropping rocks) on satellite imageries [14,15], predominantly in areas with distinct expressed lineaments, as well as in areas with intersecting/overlapping lineaments. Lineaments represent in many cases the surface expression of faults, fractures or lithologic discontinuities. Especially, when it is difficult to identify faults and lineaments in field, because of geological conditions like sedimentary covers, erosion, over-growth of vegetation, scale, and other factors, remote sensing is a valuable, additional tool. Comparisons of focal mechanisms with local neotectonic structures have shown in many cases good correlations between the orientation of nodal planes of the fault plane solutions in the depth and the orientation of fault systems observed at the surface.

The geological lineament analysis can contribute to:

- The detection of subsurface influence on macroseismic intensity in case of stronger earthquakes (reflectors of seismic waves),
- The detection of subsurface, structural influence on earthquake induced secondary effects such as slope failure,
- The inventory and analysis of faults and fracture patterns that might be relevant for surface water infiltration and rock permeability, especially in karst prone areas.

In the scope of this study mainly 3 types of linear and curvi-linear features were mapped: Lineaments, probable fault zones, and structural features. As traces of structural features were considered deformations due to stress such as synclines or anticlines, bedding structures,

foliation that become visible as dense, arc-shaped, parallel lines.

The mapped lineaments were compared then with available fault data from the USGS, and seismotectonic data, mainly with the position of earthquake epicentres, the time of earthquake occurrence, magnitude and depth.

The visibility of linear features depends on the specific properties of the satellite systems such as their spatial and radiometric resolution or acquisition time. Thus, lineament analysis was carried out in the scope of this research based on Landsat and Sentinel radar imageries, as well as on high spatial resolution BingMap_Aerial of Microsoft and World-Imagery layers provided by ESRI. Morphometric maps derived from digital elevation data such as the Shuttle Radar Topography Mission (SRTM) and Advanced Spaceborne Thermal Emission and Reflection Radiometer (ASTER) global digital elevation model (GDEM) data supported the lineament analysis by visualizing linear, morphologic features. The combined evaluation of these different satellite data allowed a more detailed inventory of the structural pattern as far as possible by the use of remote sensing tools.

2.2 Sentinel-1 and 2: Radar and Optical Data

The Sentinel radar data available since 2015 from this area covering large areas offer additional possibilities for the lineament analysis. The satellite radar data are provided by the Sentinel-1 mission, a joint initiative of the European Commission (EC) and the European Space Agency (ESA). The Sentinel-1 mission contains C-band imaging operating in four exclusive imaging modes with different resolution (down to 5 m) and coverage (up to 400 km). Although radar-foreshortening and lay-over effects have to be considered, linear, tonal features appear on the radar images, that are probably related to traces of sub-surface structures (Fig. 3). These linear features were mapped as “radar-lineaments”. Images of the Sentinel-2-satellites are available since December 2015. Sentinel-2 comprises a multispectral imager (MSI) covering 13 spectral bands (443 nm–2190 nm) with a swath width of 290 km and spatial resolutions of 10 m (4 visible and near-infrared bands), 20 m (6 red-edge/shortwave-infrared bands) and 60 m (3 atmospheric correction bands) [16].

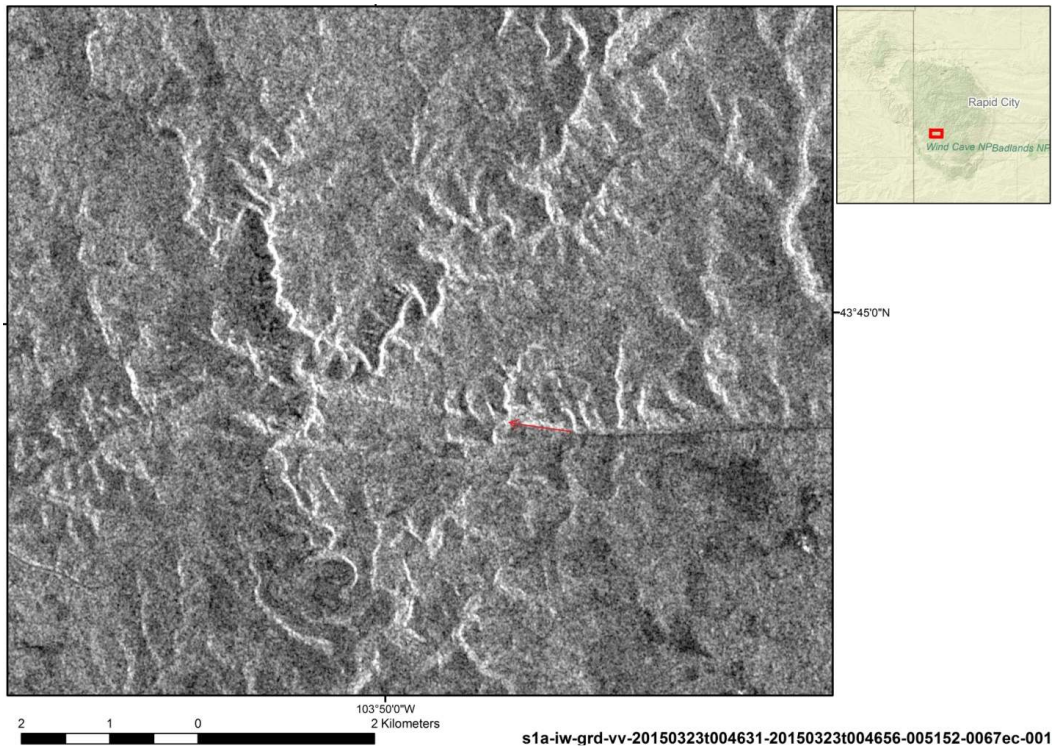

Fig. 3. Linear morphologic features visible on a Sentinel radar scene of the southwestern part of the Black Hills tracing fault zones (red arrow)

2.3 Evaluations of High Resolution Satellite Data

The high resolution satellite data provided by Google Earth form an important data input for the detailed mapping of the different types of karst phenomena in the research area. As dolines and sinkholes are often smaller than 30 m in diameter, the spatial resolution of the Landsat data is not sufficient for mapping purposes. BingMap Aerial delivered by Microsoft was another used tool and database. ESRI provides high resolution World_Imagery-layer-files.

2.4 Analysis of Digital Elevation Model Data

Morphometric maps such as slope, hillshade, height level, and curvature maps were generated based on SRTM and ASTER GDEM Digital Elevation Model (DEM) data using ArcGIS / ESRI and ENVI/ EXELIS digital image processing software. The Shuttle Radar Topography Mission (SRTM) obtained elevation data on a near-global scale to generate the most complete high-resolution digital topographic database of Earth. It is consisted of a specially modified radar system that flew onboard the Space Shuttle Endeavour during an 11-day mission in February of 2000. SRTM was an international project spearheaded by the National Geospatial-Intelligence Agency (NGA), NASA, the Italian Space Agency (ASI) and the German Aerospace Center [17]. Similarly, the Ministry of Economy, Trade, and Industry (METI) of Japan and the United States National Aeronautics and Space Administration (NASA) jointly release of the ASTER GDEM (V2) on October 17, 2011.

2.4.1 Deriving morphometric maps and extraction of morphometric factors influencing the susceptibility to natural hazards

From SRTM and ASTER GDEM (both 30 m spatial resolution) data derived morphometric maps (slope gradient maps, drainage, etc.) were combined with lithologic and seisomotectonic information in a GIS integrated data base. The GIS integrated geospatial geodata analysis was used to detect, map and visualize factors that are known to be related to the occurrence of higher earthquake shock and/or earthquake induced secondary effects [18,19].

When searching for areas susceptible to soil amplification, liquefaction or compaction the so called causative or preparatory factors have to be taken into account such as height levels, slope gradients, terrain curvature, lithologic conditions and faults zones. Morphometric properties of an area can influence to a great deal local site effects during earthquakes and earthquake related secondary effects. Various factors can be extracted from DEM data that might be of importance for the detection of local site conditions influencing earthquake ground motion such as:

- Height level maps help to search for topographic depressions covered by almost recently formed sediments, which are usually linked with higher groundwater tables. When extracting the lowest height level of an area, it becomes visible where the areas with high ground-water tables can be expected. In case of earthquakes those areas have often shown the highest earthquake damage intensities. From the DEM data flat areas with no curvatures of the terrain, low to no slope gradients and the lowest areas were extracted.
- Slope gradient maps help to detect areas where mass movements are likely to occur. From slope gradient maps are extracted those areas with the steepest slopes, and from curvature maps the areas with the highest curvature as these are susceptible to landslides. Slopes with higher slope gradient are generally more susceptible to mass movements. Slope gradients < 10° indicate flat areas, often covered by unconsolidated, youngest sediments.

Morphometric conditions play an important role as well for the detection of areas susceptible to flash floods [20]. The lowest and flattest areas show in general the highest disposition to be flooded.

2.4.2 Weighted overlay

An important step towards susceptibility mapping is the weighted overlay method in ArcGIS allowing the aggregation and weighting of causal factors influencing the susceptibility to natural hazards. The analysis method and integration rules can easily be modified in the GIS architecture as soon as additional information becomes available [4].

For example: The influence of the factors on earthquake ground motion is not equally

important in the analysis. The percentage of influence of one factor might be changing, for example due to seasonal and climatic reasons, or distance to the earthquake source. As a stronger earthquake during a wet season will probably cause more secondary effects than during a dry season, the percentage of its influence has to be adapted. In very hot and dry seasons the risk of liquefaction or landslides is generally lower than in spring times. This seasonal influence on earthquake effects has to be taken into account and should be monitored systematically. The sum of all factors / layers, that can be included into the GIS, provides information of the susceptibility to amplify seismic signals. As geotechnical measurements in the field are time and cost intensive the available remote sensing and GIS data and tools can help to prepare and plan these investigations more focused. The weighted overlay for this study was carried out using mainly the causal, morphometric factors (Fig. 4).

3. REMOTE SENSING AND GIS EVALUATION RESULTS FOR THE DIFFERENT NATURAL HAZARDS

The next chapter comprise examples for the contributions of remote sensing and GIS or the detection of causal factors influencing the development and intensity of the impact of the different natural hazards.

3.1 Seismic Hazards

Earthquakes affecting the Black Hills area have been documented [21,22,23], recording events with magnitudes of 3.5 and above up to 5 (Fig. 5).

At least two mechanisms may be important in generation of these earthquakes. These include initiation of movement along partly pre-existing faults and fractures due to crustal plate movements or movements due to glacial rebound.

When comparing earthquake data of the last decades from South-Dakota and Wyoming considering the months of occurrence and their depth (km), it is obvious that the majority of earthquakes below 10 km depth happen after the humid months from June to August, partly September (Fig. 6). Most of the major earthquakes are recorded in the post-humid period. Earthquakes below 10 km depth are concentrated in the months November and December, implying a time delay between the surface water infiltration along major fault and fracture zones and earthquake triggering effects?

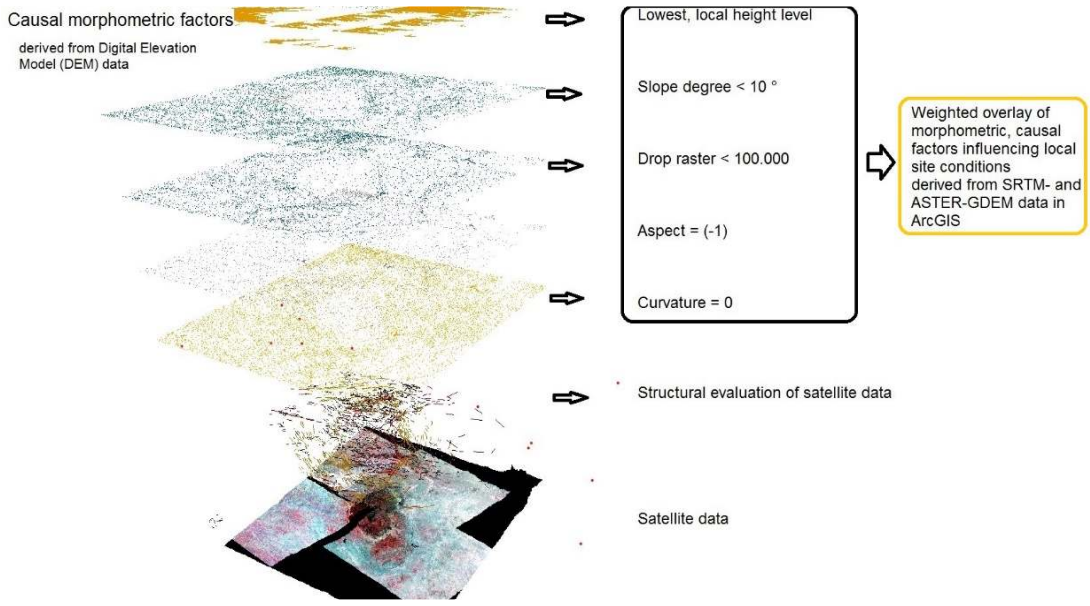

Fig. 4. Weighted overlay of causal, morphometric factors influencing the susceptibility to soil amplification

(Such as local, lowest height levels, lowest slope degrees < 10°, curvature = 0, flat-test areas)

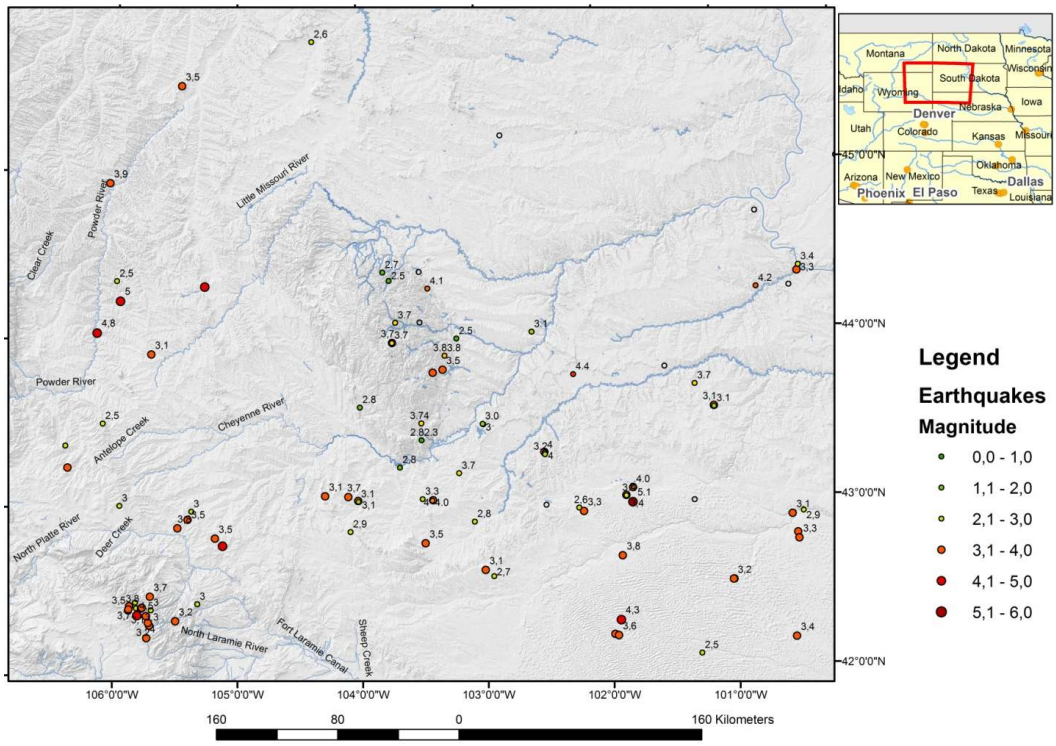

Fig. 5. Earthquake epicenters [21,22]

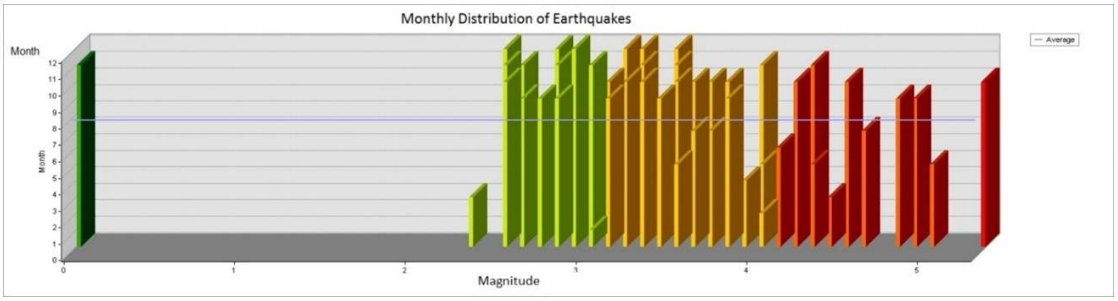

Fig. 6. Earthquake monthly occurrence

The structural evaluation of Landsat 8 data was combined with satellite radar images. A combined approach of evaluating multispectral and radar data provides advantages over individual use of either sensor. The digital image processing of Landsat and Sentinel radar data enhanced structural features surrounding the central uplift. The evaluations of Landsat 8 data clearly reveal that the structure of the Black Hills is far more extended than visible in the surficial landscape. Traces of the structural features are ranging in width about 260 km and in length nearly 400 km. The earthquakes during the last decades seem to occur concentrated along the outer rim of the Black Hills uplift structure and the southeastern flank. This might indicate ongoing tectonic processes such as uplift (Figs. 7, 8).

The combined lineament analysis contributes to the more detailed inventory of the structural pattern in the Black Hills. The evaluation of Sentinel radar images supports the detection of distinct expressed linear features are often related to fault and fracture zones. The illumination geometry of the radar signals plays an important role for the visibility of the features. Linear features perpendicular to the radar illumination appear very clearly, linear features parallel to the illumination are often suppressed. In spite of the radar shadows and layover effects

larger fault zones can be detected, especially because of their small-scale roughness of the radar backscatter. These were mapped as lineaments (Fig. 9b).

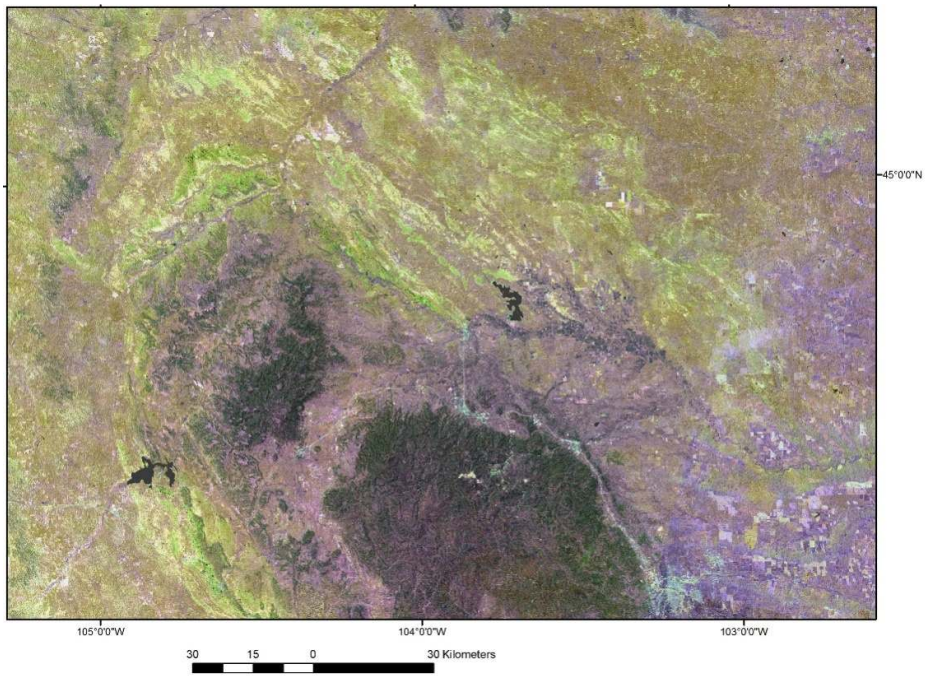

Fig. 7. Landsat 8-mosaic of band combinations 6,1,5 and 8 showing subsurface structures of the northern part of the Black Hills resulting from updoming of the strata

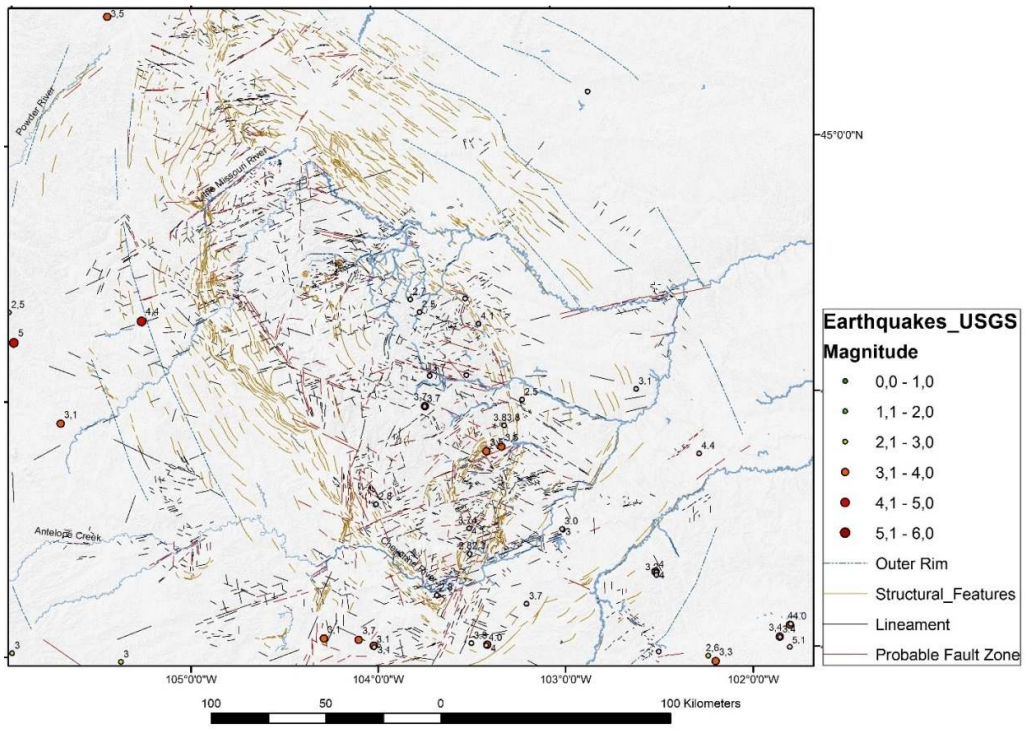

Fig. 8. Structural evaluation of Landsat-data (lineament analysis)

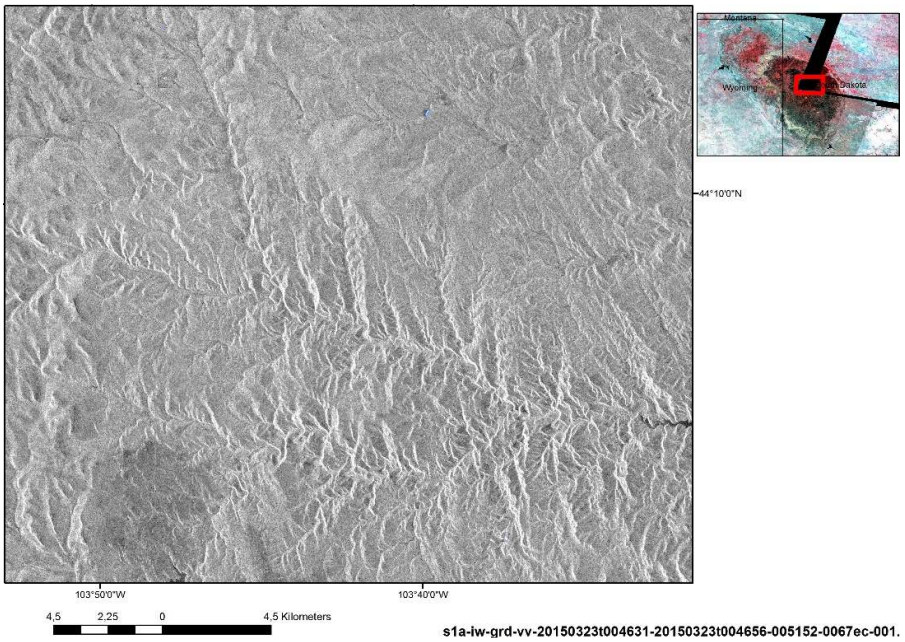

(a)

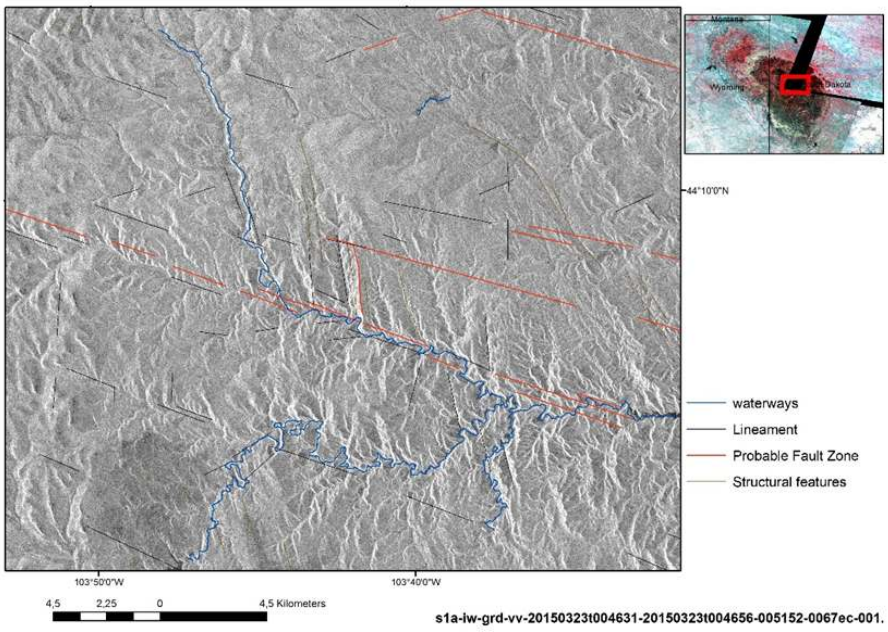

(b)

Fig. 9a and b. Fault zone visible on a sentinel radar scene

The radar illumination from west to east enhances westwards oriented slopes in light gray tones due to the stronger reflection of radar signals along the western slopes

As one of the prerequisite for earthquake preparedness in the area of the Black Hills an inventory of sites more susceptible to earthquake damage and to earthquake related secondary effects due to local site conditions should be carried out.

The inhomogeneous spatial distribution of damage caused by earthquakes is above all controlled by the local geological conditions that can amplify or de-amplify the amplitude of the seismic motion before it reaches the surface of the ground or the foundation of the buildings. The effect of the local conditions over the ground motion is determined by the way in which the seismic waves, during the propagation from the bedrock to the ground surface, are affected by the structure and the geometry of deposits from above. The ground-shaking during an earthquake predominantly depends on several factors such as the magnitude, properties of fault plane solutions, the distance from the fault and local geologic conditions. The most intense shaking experienced during earthquakes generally occurs near the rupturing fault area, and decreases with distance away from the fault. Within a single earthquake event, however, the shaking at one site can easily be stronger than at another site, even when their distance from the ruptured fault is the same. The variability in earthquake-induced damage is mainly determined by the local lithological properties, thickness of the soil and lithologic unit layer, by hydrogeological, structural and by geomorphological conditions. These conditions, intern influence the amplitude, the frequency and duration of ground motion at a site [24,25].

Groundwater level variations and associated saturation changes in sand layers within near-surface aquifers can influence local response spectra of the ground motion through modification of shear-wave velocity. Recently formed sediments will slow the velocity of the earthquake waves, trapping the energy and causing large amplitudes of shaking. Older compacted materials that over time have densified or transitioned from sand to sandstone and cemented together are less responsive for example to liquefaction. Changes of the groundwater level can have a considerable influence upon the liquefaction potential of a region due to in-situ pore-water pressure responses in aquifers during earthquakes triggering mechanism of liquefaction [25,26].

The evaluations of the weighted overlay result aggregating and weighting causal, morphometric and geologic factors support the assumtion that the Black Hills area is affected by soil amplification mainly along broader riverbeds due to local site conditions (Fig. 10).

The example of the area of Rapid City shows how the weighted overlay of morphometreic, causal factors combined with geologic information such as the outcrop of unconsolidated, youngest sediments can contribute to the detection of local site conditions. Comparing the results of the weighted overlay-calculations with geologic maps, there is a clearly visible coincidence of areas with higher susceptibility values and the outcrop of unconsolidated, Quaternary sediments in valleys and depressions (Fig. 11).

Whenever stronger earthquakes happen in this area, based on the existing reference data base it can be derived better, where relatively higher damages are more likely to occur. Thus, remote sensing data and GIS integrated evaluation and analysis can contribute to a better planning of cost and time-intensive geotechnical measurements that are important to consider. So far no detailed available, macroseismic observation and records could be used confirming these remote sensing based results in the Black Hills region. However, the good correlation and coincidence between the weighted overlay results and macroseismic records in other countries such as in Greece or Japan verify this approach [4]. Higher macroseismic intensities during stronger earthquakes were observed exactly in those areas where in the weighted overlay maps showed the highest susceptibility to ground motion.

3.2 Flash Floods

Flash floods after high precipitations within short times causing flooding of riverbeds and lowlands with high damages have occurred repeatedly in the areas surrounding the Black Hills. On June 9-10, 1972, extremely heavy rains over the eastern Black Hills of South Dakota produced record floods on Rapid Creek and other streams in the area. Nearly 15 inches of rain fell in about 6 hours near Nemo, and more than 10 inches of rain fell over an area of 60 square miles. The resulting floods left 238 people dead and 3,057 people injured. Runoff from this storm produced record floods (highest peak flows recorded) along Battle, Spring, Rapid, and Boxelder Creeks. Smaller floods also occurred along Elk Creek and Bear Butte Creek [27].

The Weighted Overlay Tool in ArcGIS for flooding susceptibility-approach is summarizing causal / preparatory factors influencing flooding susceptibility. Causal factors were extracted from morphometric maps that might be of importance

for the detection of local site conditions influencing the disposition to flooding hazards. Such causal factors are

- Relatively lowest local height levels,
- Slope gradients < 10°,
- Minimum terrain curvature (values=0 corresponding to flat terrain),
- Drop raster < 100.000 (The dropraster is calculated using the Hydrology tools of ArcGIS. It is calculated as the difference in z-value divided by the path length between the cell centers, expressed in percentages. For adjacent cells, this is analogous to the percent slope between cells. The result is a map of percent rise in the path of steepest descent from each cell.),
- Flat areas derived from aspect maps (extraction of values [-1]) and
- High flow accumulation values.

These causal factors were aggregated and weighted [26,28], in this case starting with equal influence.

The weighted overlay of these morphometric properties and factors enhancing the susceptibility to inundation provides an overview

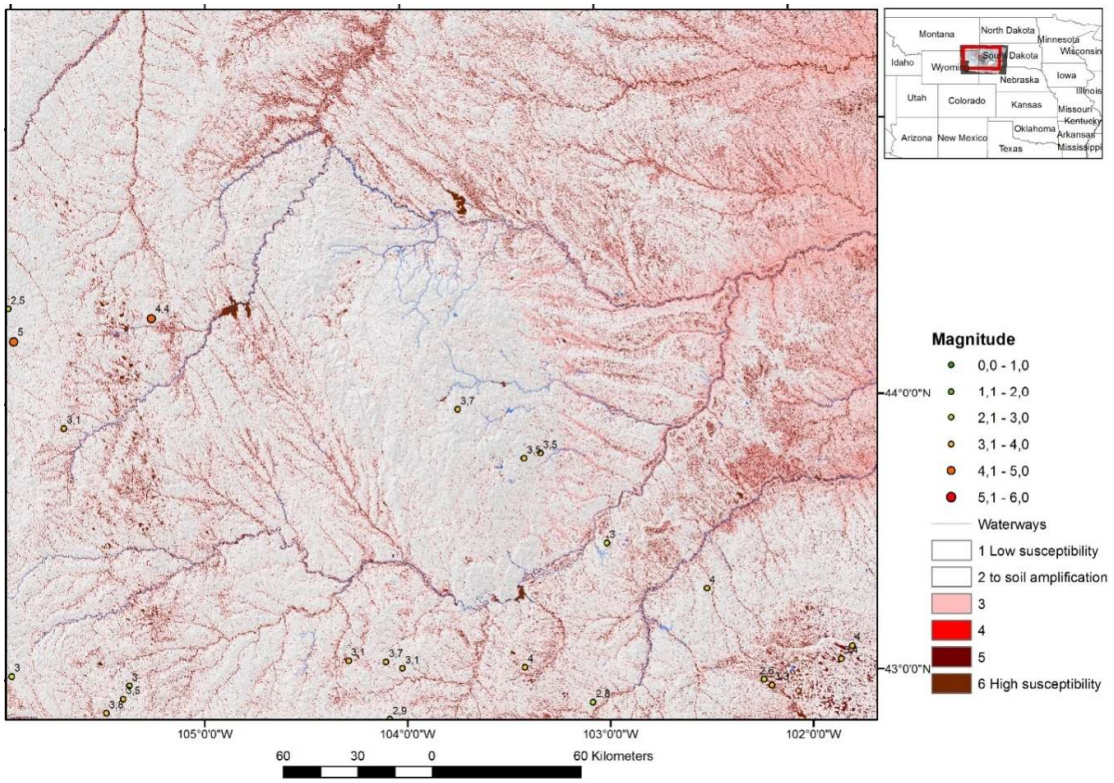

Fig. 10. Weighted overlay of morphometric factors derived from ASTER DEM data

Morphometric Maps ➡ Extraction of Causal Factors ➡ Aggregation / Weighted Overlay

Height Level maps Slope Degree Curvature Aspect	Local, lowest height levels lowest slope degrees < 10° curvature = 0 flattest areas (-1) dropraster < 100.000	Influence (%) varying according to seasonal changes, calculated in this case with equal influence

Dark red areas are correlated with the relatively higher susceptibility to earthquake ground motion due to their morphometric properties and disposition (such as broader valleys, depression with outcropping unconsolidated sediments). Aggregation and overlay of morphometric factors in ArcGIS such as: slope < 10°, curvature =0, aspect = (-1), dropraster < 100.000 (weight: equal influence), method according to [26]

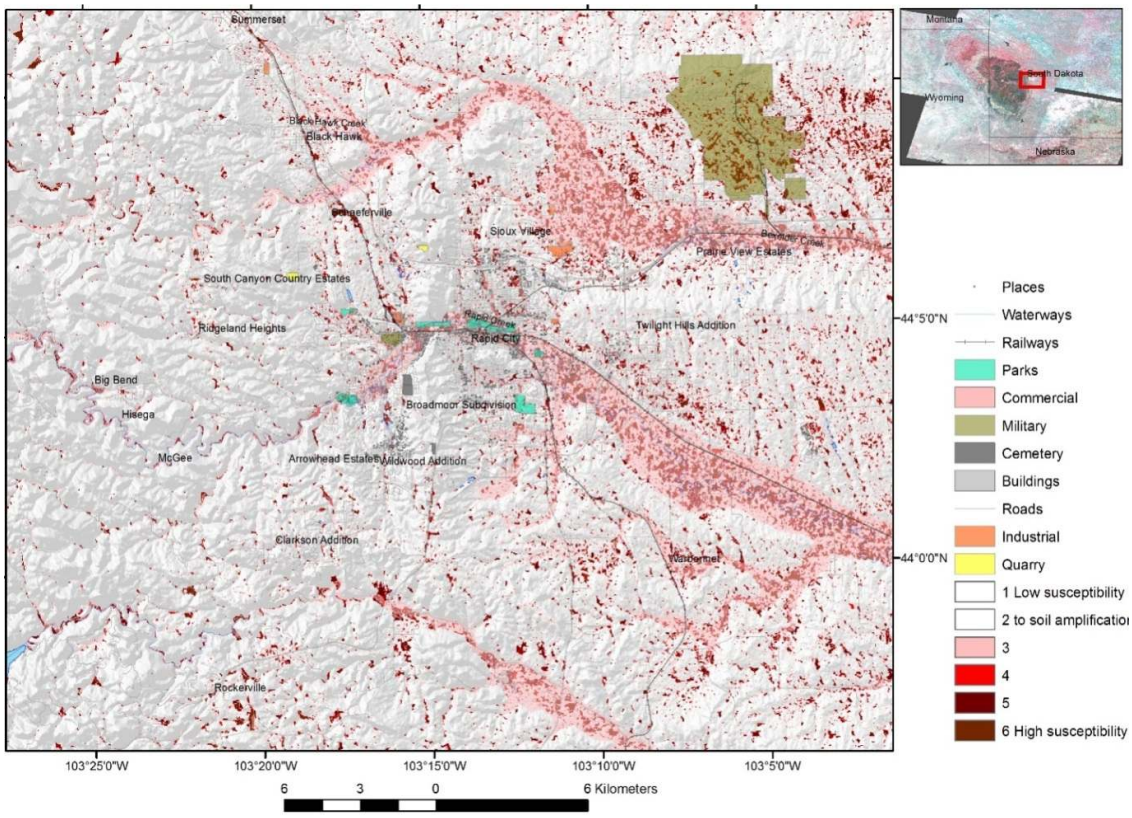

Fig. 11. Weighted overlay of morphometric factors influencing local site conditions combined with the layer of the outcrop of Pleistocene and Holocene provided by USGS

map indicating, where these factors sum up and interfere each other. The resulting maps are divided into susceptibility classes. The susceptibility to flooding is classified by values from 0 to 6, wherein the value 6 is standing for the highest, assumed susceptibility to flooding due to the aggregation of the causal / preparatory factors. The areas with the highest susceptibility to be affected by flooding due to their morphometric properties and disposition are presented in dark-blue. Whenever the above mentioned causal factors occur aggregated in this area, the susceptibility to extreme flooding events such as flash floods is rising as the local lowest and flattest areas are generally prone more to flooding than the environment.

A more detailed result is shown in Fig. 12b for the area of Rapid City. Those areas that might be prone to a relatively higher flooding susceptibility due to their morphometric disposition are clearly visible (dark-blue). Such maps could be useful for local emergency authorities when dealing with flash flood preparedness and land use planning. Within the areas (dark-blue in Fig. 12b) indicating a higher flooding susceptibility there are parks in Rapid City (green on Fig. 12b), revealing the awareness of the potential flooding hazard.

The results of the weighted overlay were compared with the flood data of FEMA [29] (delivered as shapefiles) revealing a clear coincidence of areas with the highest susceptibility to flooding and flooded areas in the past (100 years flood events). Of course, many factors play a role when dealing with flash floods such as the precipitation intensity, the size of catchment areas, morphologic watersheds, lithologic conditions, vegetation cover or land use. The results of the weighted overlay using morphometric parameters help to delineate those areas with a morphometric disposition to be flooded (Fig. 13).

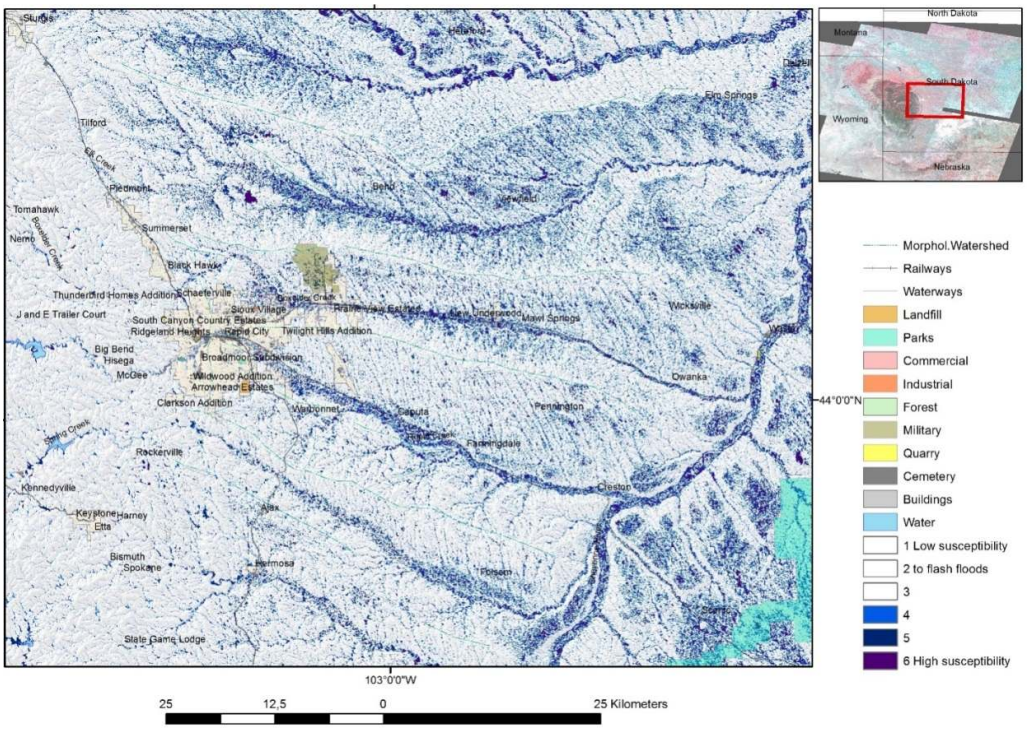

Fig. 12a. Weighted overlay of causal morphometric factors influencing the susceptibility to flash floods along the eastern border of the Black Hills

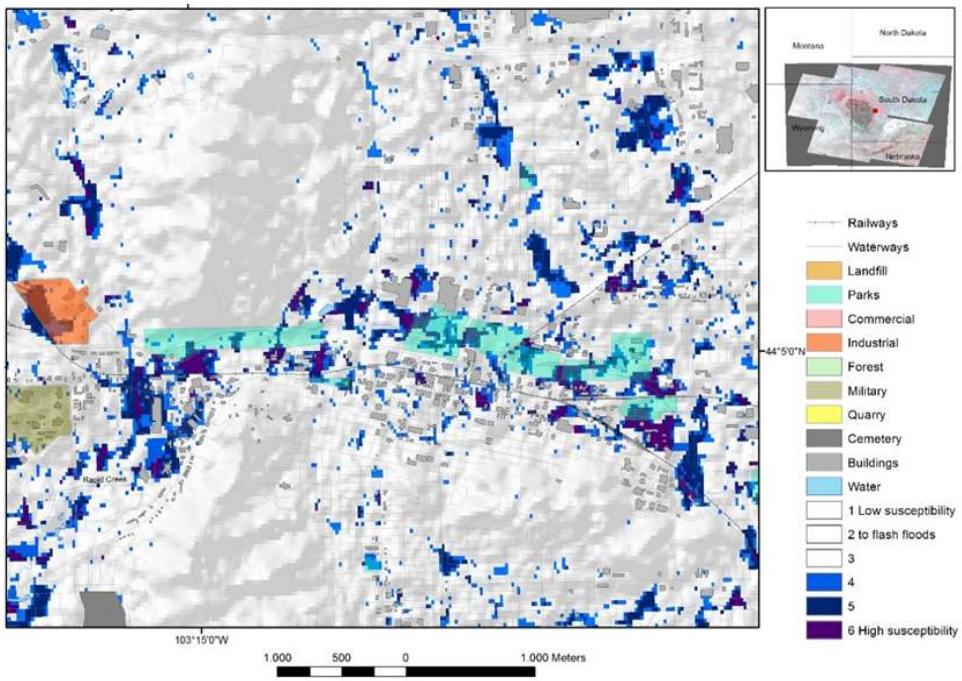

Fig. 12b. Weighted overlay of causal morphometric factors influencing the susceptibility to flash flood inundation in Rapid City

The weighted overlay of morphometric properties such as slope degrees < 10°, curvature = 0, aspect = (-1), dropraster < 100.000, local lowest height level, and flow accumulation

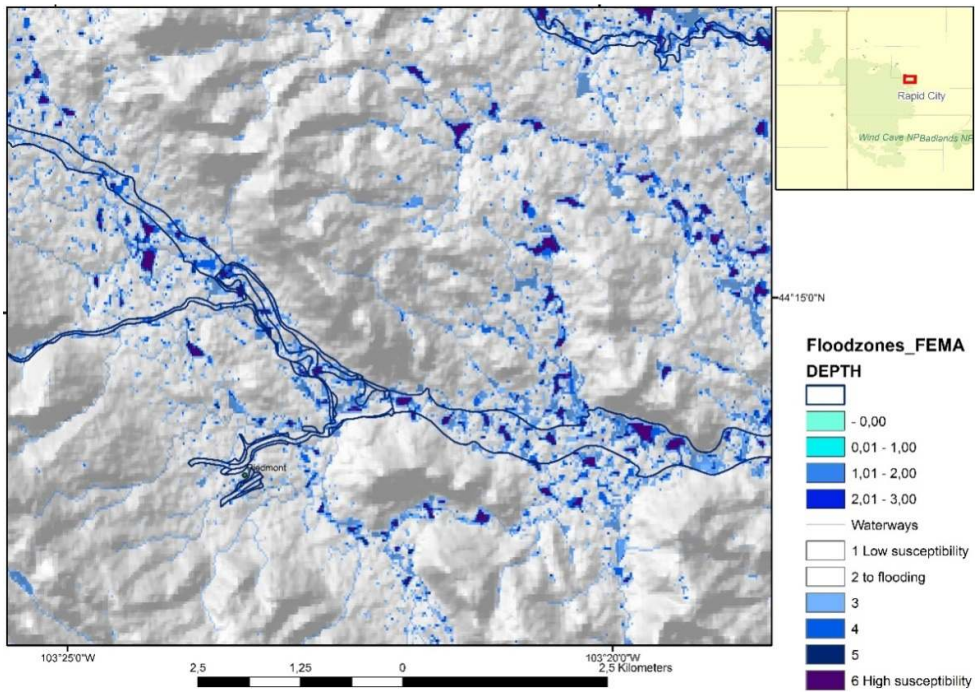

Fig. 13. Comparison of the outlines of past flooding events [29] with the weighted overlay results indication areas with high susceptibility to flooding due to their morphometric disposition

3.3 Karst Phenomena

The occurrence of karst phenomena and their continual evolution can pose serious problems related to subsurface stability and may require caution in the maintenance and planning of infrastructure in the area of the Black Hills. Therefore caution in land use planning is required, in due to damage to buildings, roads, water supply systems and in rural areas through the loss of arable land. Thus, when dealing with the construction and maintenance of infrastructure (highways, pipelines, sewage), areas of high intensity karst development should be carefully monitored. Effects of long-term destabilization processes on subsurface stability by dissolution processes and sinkhole formation along pre-existing fracture and fault zones in combination with hydrologic (high precipitation) and with tectonic triggering factors (neotectonic movements), as well as with earthquakes pose important research issues in this area.

Karst development commonly occurs within sections of three formations in the Black Hills region. The oldest karst features occur in the Mississippian Madison Limestone, a limestone-dolomite system that exhibits a karsted surface as well as extensive cave formation. The Pennsylvanian-Permian Minnelusa Formation contains anhydrite and thin limestone beds that have undergone localized and varied karstification. Hydration and swelling of primary anhydrite has resulted in multiple collapse structures within the formation. The Triassic Spearfish Formation contains gypsum deposits throughout; however, massively bedded gypsum up to 10 m thick is contained at the top in the Gypsum Spring Member [30,31,32,33].

Dissolution of gypsum and anhydrite in four stratigraphic units in the Black Hills, South Dakota and Wyoming, has resulted in development of sinkholes. Subsidence has caused damage to houses and water and sewage retention sites. Substratal anhydrite dissolution in the Minnelusa Formation (Pennsylvanian and Permian) has produced breccia pipes and pinnacles, a regional collapse breccia, sinkholes, and extensive disruption of bedding. Anhydrite removal in the Minnelusa probably dates back to the early Tertiary when the Black Hills was uplifted and continues today. Evidence of recent collapse includes fresh scarps surrounding shallow depressions, sinkholes more than 60 feet deep, and sediment disruption and contamination in water wells and springs [30,31]. Anhydrite removal in the

Minnelusa probably dates back to the early Tertiary when the Black Hills area was uplifted and continues today. Evidence of recent collapse includes fresh scarps surrounding shallow depressions, sinkholes more than 60 feet deep, and sediment disruption and contamination in water wells and springs. The karst-typical landforms like the dolines, partly occurring as uvalas, were identified on satellite and aerial imageries due to their characteristic morphologic properties and circular to oval outline. Numerous dolines and smaller depressions were found, some of them surely not known yet, although errors in the scope of the remote sensing evaluation process cannot be excluded. Partly the mapped dolines could be verified by field research (Figs.15, 16) [30,31].

The visibility of dolines on satellite images depends on seasonal influences what makes standardized approaches of digital image processing difficult. Smaller depressions are often only visible on the satellite imageries and aerial photographs due to subtle, tonal differences, expressed as darker, almost circular shaped features. During wet seasons sinkholes are more expressed on the images due to higher photosynthetic activity and soil moisture or water fill. Circular features with about 1 km in diameter were detected on the satellite images with uncertain origin (Fig. 15). Whether they might be explained by sinkhole-origin remains to further investigations.

The pattern and surface alignments of karst features in the study area are structurally controlled and associated with subsurface structures such as joint patterns, faults and folding. This relationship can be visualized by the structural evaluation of remote sensing data. The dolines visible on Fig. 16 are aligned exactly on a lineament.

The development of karst phenomena depends on the ability of water to sink into and flow through karst rocks. The amount of limestone affected by dissolution during the karstification processes mainly depends on the amount and the concentration of the dissolution [32,33]. Whenever water percolates through the fractures and fissures, these openings become enlarged through dissolution, and water transport increases. Thus, it can be assumed, that in the areas with higher surface water input and following infiltration the karstification processes are more intense [34]. Therefore the investigations were focused on the detection of areas with higher surface water input after precipitations and on areas with distinct visible lineaments.

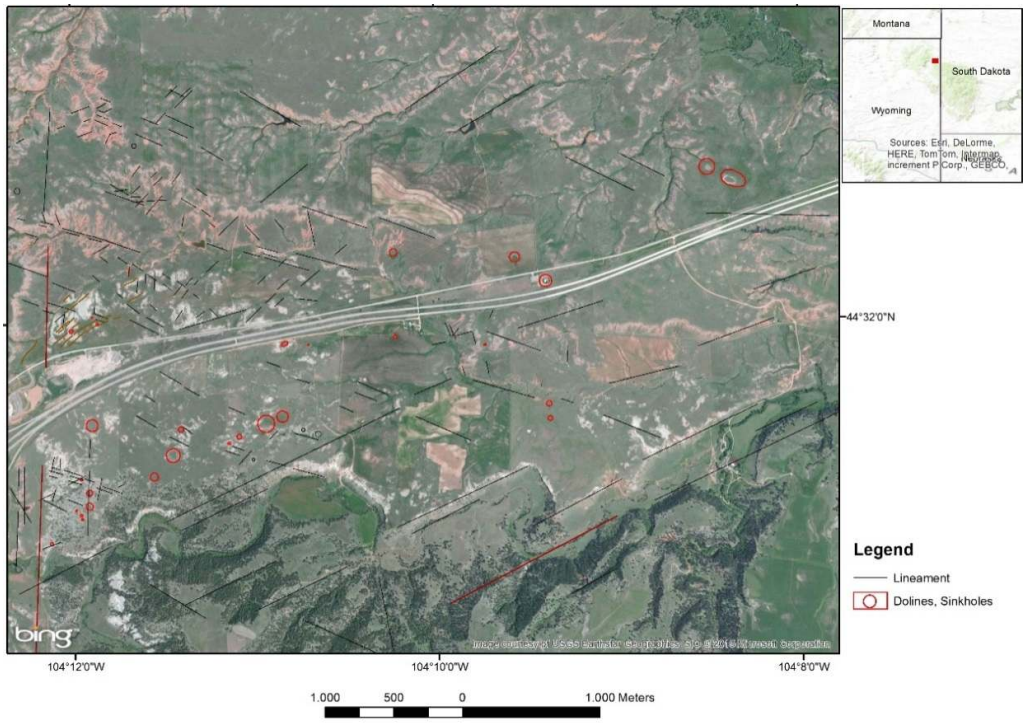

(a)

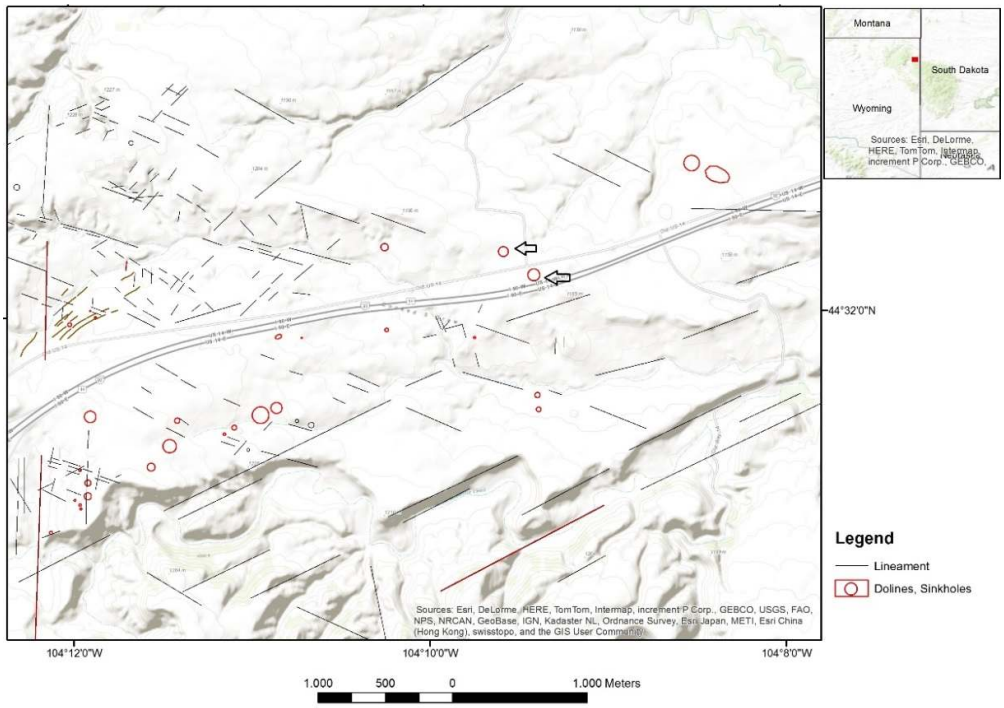

(b)

Fig. 14a and b. Mapping of circular and oval features assumed to be related to sinkholes and lineament analysis

The two dolines with arrows are verified by field research [30]. The upper one, the "Vore Buffalo Jump", is an 18-m deep sinkhole

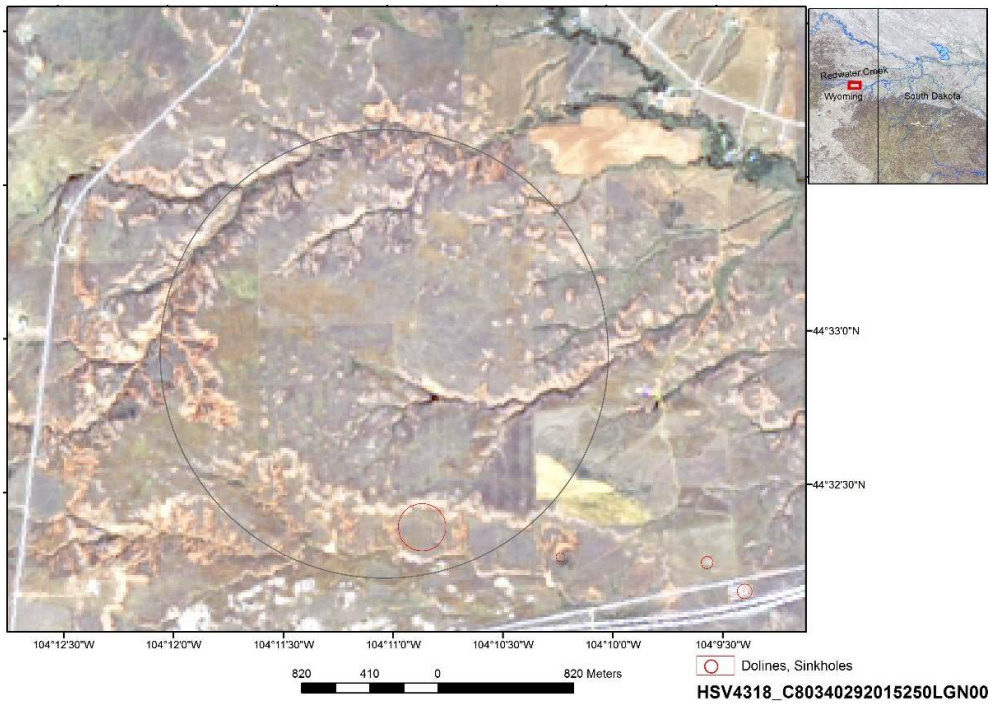

(a)

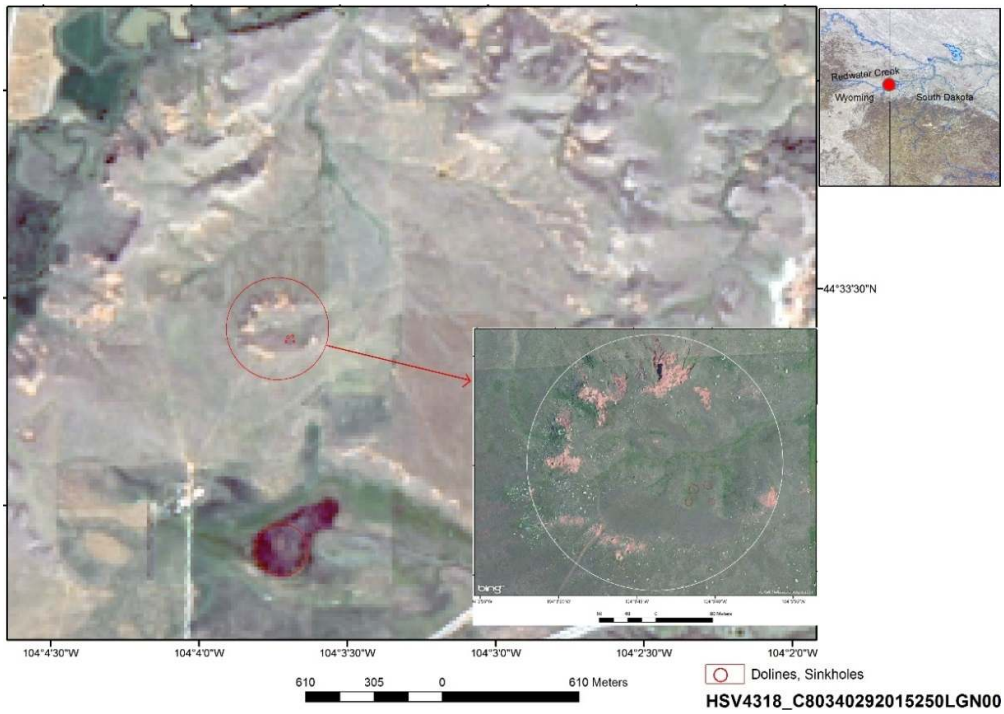

(b)

Fig. 15a and b. Circular structures visible on Landsat 8 and BingMap_Aerial-scenes

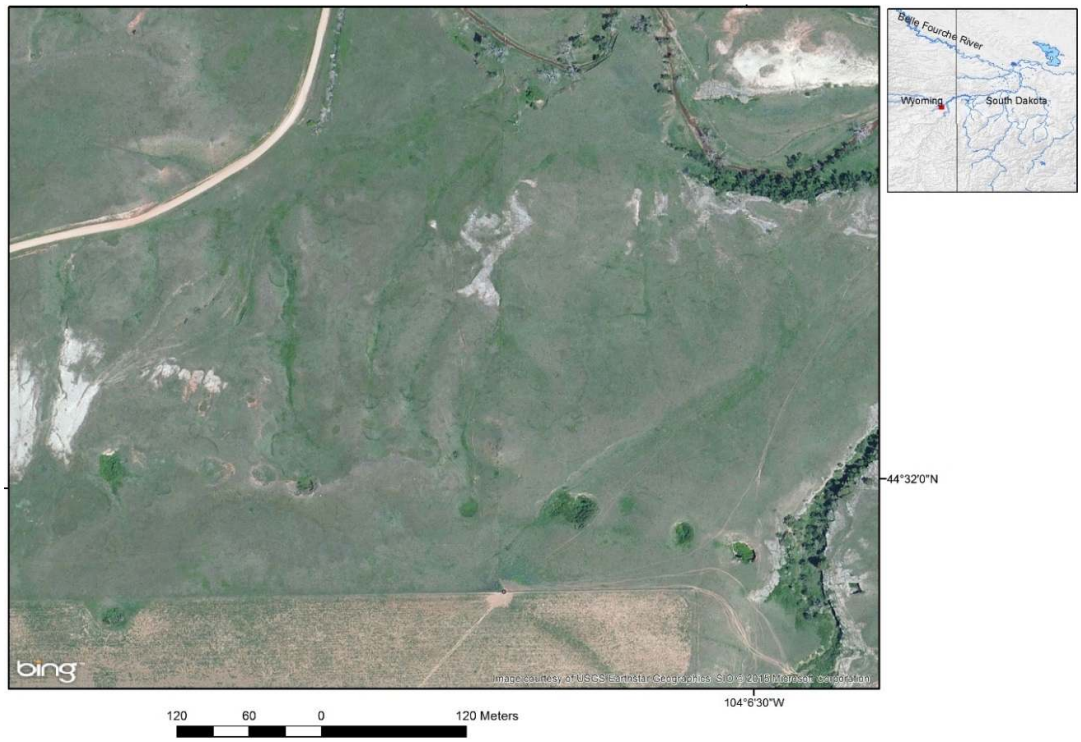

Fig. 16. Dolines tracing linear subsurface structures as visible on a BingMaps_Aerial-scene

As the morphometric analysis of digital elevation data helped to visualize the small-scaled variations at the surface, characterized by subtle changes of depressions and elevations, from SRTM and ASTER Digital Elevation Model (DEM) data derived morphometric maps (slope gradient maps, height level, drainage, etc.) were used for the detection of karst phenomena. However, the majority of the dolines are less than 100 m in size. They are often smaller than the 30 m spatial resolution of SRTM DEM and ASTER GDEM data and therefore not visible on the from satellite DEM data derived morphometric maps.

When searching for areas relatively more susceptible to karst processes than the environment due to higher surface water input, the so called causal factors have to be taken into account that might be of influence. As the lowest and flattest areas are prone to higher amounts of surface water input, the overlay of morphometric factors (lowest local height level, lowest dropraster values, slope degree < 10°, curvature=0) helped to identify those regions. Fig. 17 shows the results of the weighted overlay merged with the map of doline / sinkhole occurrence, lineaments and lithologic information.

4. CONCLUSIONS

By using remote sensing and GIS methods a systematic, standardized inventory of areas around the Black Hills has been carried out that are more susceptible to natural hazards like flash floods, higher earthquake ground motions, or karst phenomena. The presented study has demonstrated that the creation of a basic, standardized data stock is possible with relatively low financial resource input when using the open-source data and information and Web-gateways, especially those of the USGS.

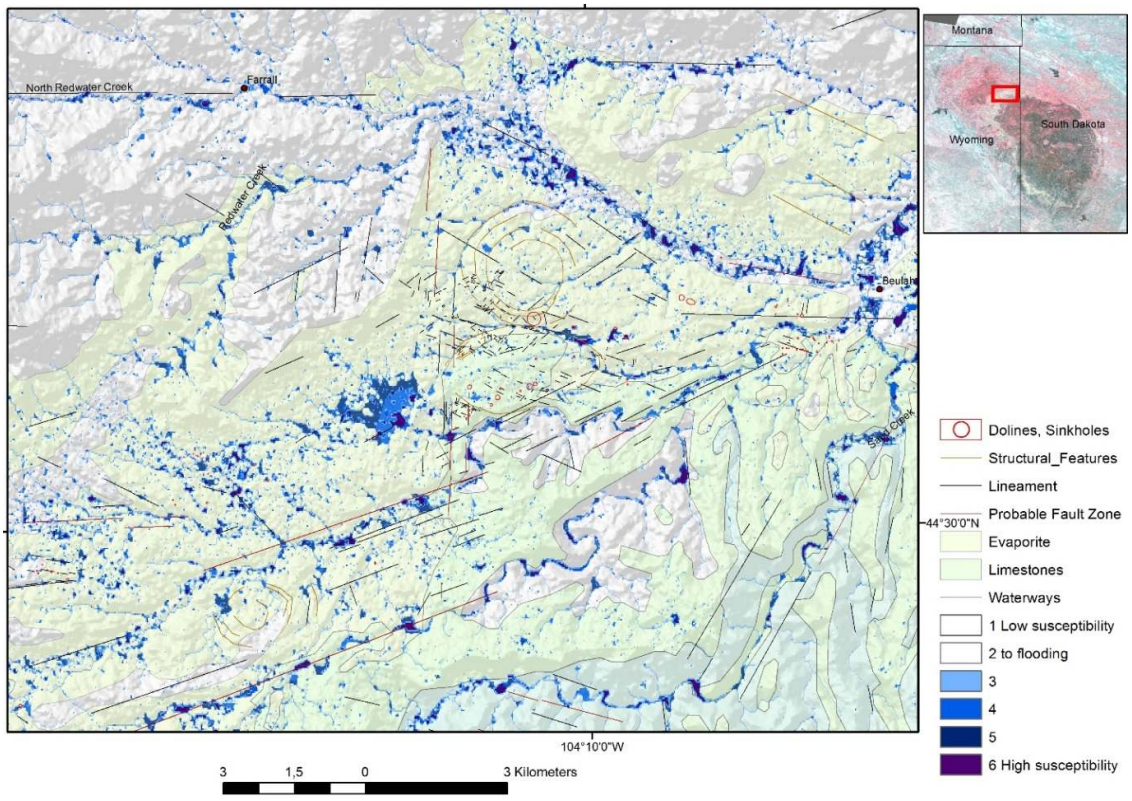

Fig. 17. Factors influencing the development of karst phenomena

- *Occurrence of the majority of dolines / sinkholes within the outcrops of evaporates, dolomites and limestones.*
- *Susceptibility to a relatively higher surface water input after rainfall due to the morphometric disposition (dark-blue - lowest and flattest areas) influences dissolution processes.*
- *Intersecting, larger fault zones enhancing the permeability of the rocks and the susceptibility to collapse*

The evaluations of satellite imageries such as Landsat, Sentinel, digital topographic data and of open-source geodata contribute to the acquisition of the specific tectonic, geomorphologic/topographic settings influencing earthquake ground motion due to local site conditions in case of stronger earthquakes. After weighting the factors according to their probable influence on ground shaking susceptibility maps were elaborated, where those areas were considered as being more susceptible to higher earthquake shock intensities, where "negative" factors occur aggregated and interfering with each other. Whenever an earthquake happens in these areas, now it can be derived better where the "islands" of higher ground shaking are most likely to occur by adding the specific information of the earthquake to the susceptibility map using the weighted overlay – approach.

The hereby presented approach is proposed to serve as a first basic data stock for getting a perception of potential sites susceptible to higher earthquake ground motion, including then in next steps the integration of further, available data such as movements along active faults, focal planes, 3D structure, lithologic properties and thickness of lithologic units, etc.

The weighted overlay approach in ArcGIS supports the delineation of affected areas by aggregating and summarizing causal factors characterizing flash flood areas. Whenever a flash flood event happens in the Black Hills area, it can be derived from the elaborated database, which areas might be prone more to these geo-hazards than the environment due to their specific morphologic disposition. This could be confirmed by continuously, long-term monitoring.

GIS integrated evaluations of different satellite data can contribute considerably to the detection of subsurface structures in the Black Hills area. Satellite imageries serve as georeferenced base for the mapping of linear features, obviously related to subsurface structures and, thus, contributing to the structural inventory.

Lineament maps are providing hints where the intrusion and infiltration of surface water into the subsurface might be more intense due to fracture zones within the outcropping rocks and, thus, influencing karstification processes, especially in the northern part of the Black Hills. The alignment of dolines along fracture and fault zones is clearly visible on high resolution satellite and aerial images.

When combining the results of the weighted overlay of morphometric factors influencing the susceptibility to relatively higher surface water input and flooding, the results of the lineament analysis and the results of the inventory of dolines and sinkholes, a better understanding and visualizing of some of the different factors influencing the development of karst phenomena can be achieved. By systematically and continuously compiling this knowledge and available resources, by implementing the data into a widely accessible database and by raising awareness for this potential geohazard (subsurface instability), land use planning in this area can be supported.

COMPETING INTERESTS

The author has declared that no competing interests exist.

REFERENCES

1. South Dakota Chamber of Commerce and Industry. Business continuation series: Natural disastersi. September Newsletter, 2001;1:6.
   Accessed 29 November 2015.
   Available:http://www.sdchamber.biz/media/2010sdchamberbiz//naturaldisasters.pdf
2. Department of Public Safety, SD. Accessed: 6 October 2015.
   Available:https://dps.sd.gov/emergency_services/emergency_management/hazard_vulnerability.aspx)
3. USA.com. Accessed: 7 October 2015.
   Available:http://www.usa.com/south-dakota-state-natural-disasters-extremes.htm
4. Theilen-Willige B, Savvaidis P, Tziavos IN, Papadopoulou I. Remote sensing and GIS contribution to the inventory of infrastructure susceptible to earthquake and flooding hazards in NE-Greece. Geosciences. 2012;2(4):203-220.
   DOI: 10.3390/geosciences2040203
   Available:http://www.mdpi.com/2076-3263/2/4/203
5. Driscoll DG, Hamade GR, Kenner SJ. Summary of precipitation data for the black hills area of South Dakota, water years 1931-98. U.S. Department of the Interior, U.S. Geological Survey, Open-File Report 00-329, Prepared in cooperation with the South Dakota Department of Environment and Natural Resources and the West

Dakota, Water Development District. 2000; 329:151.
(Accessed 14 December 2015)
Available:http://sd.water.usgs.gov/pubs/reports/ofr00-329.pdf

6. WorldClim – Global Climate Data. Accessed: 5 September 2015.
Available:http://www.worldclim.org/tiles.php?Zone=12
7. Lisenbee AF. Laramide structure of the Black Hills uplift, South Dakota-Wyoming-Montana. Geological Society of America, Memoir 151. 1978;165-196.
8. Lisenbee AL. Tectonic history of the black hills uplift in thirty-ninth field conference guidebook, Eastern Powder River Basin – Black Hills. Casper, Wyoming: Wyoming Geological Association; 1988.
Available:http://pbadupws.nrc.gov/docs/ML1302/ML13023A327.pdf
9. Dewitt E, Redden JA, Burack Wilson A, Buscher D, Dersch JS. Mineral resource potential and geology of the black hills national forest, South Dakota and Wyoming. U.S. Geologicl Survey Bulletin 1580; 1986.
(Accessed: 15 November 2015)
Available:http://pubs.usgs.gov/bul/1580/report.pdf
10. Redden JA, DeWitt E. Maps showing geology, structure, and geophysics of the Central Black Hills, South Dakota. U.S. Geological Survey Scientific Investigations Map 2777, 44-p. pamphlet, 2 sheets.
Available:http://pubs.usgs.gov/sim/2777/downloads/2777_pamphlet_508.pdf
11. Wicks JL, Dean SL, Kulander BR. Regional tectonics and fracture patterns in the Fall River Formation (Lower Cretaceous) around the Black Hills foreland uplift, western South Dakota and northeastern Wyoming. Geological Society, Special Publications. 1999;169: 145-165.
DOI: 10.1144/GSL.SP.2000.169.01.11
12. Diffendal RF. Geomorphic and structural features of the Alliance 1° x 2° Quadrangle, western Nebraska, discernible from synthetic-aperture radar imagery and digital shaded-relief maps Contributions to Geology, University of Wyoming.1994;NRC-027, 30(2):137-147.
13. Shurr GW, Ludvigson GA, Hammond RH. Perspectives on the Eastern Margin of the Cretaceous Western Interior Basin. Geological Society of America. 1994; Special Paper, 287:43-78.
(Accessed: 3 January 2016)
Available:http://www.sdgs.usd.edu/pubs/PAPERS_PUBLICATIONS/Perspectives%20on%20the%20Eastern%20Margin%20of%20the%20Cretaceous%20Western%20Interior%20Basin/Perspectives%20on%20the%20Eastern%20Margin%20of%20the%20Cretaceous%20Western%20Interior%20Basin%20-%20Introductory%20Remarks.pdf
14. Burnett AW, Schumm SA. Alluvial river response to neotectonic deformation in Louisiana and Mississippi. Science. 1983; 222:49–50.
15. Yang CB, Chen WS, Leh-Chyun Wu, Chii-Wen Lin. Active deformation front delineated by drainage pattern analysis and vertical movement rates, southwestern coastal plain of Taiwan. Journal of Asian Earth Science. 2007;31:251–264.
16. ESA: Facts and Figures. Accessed 10 December. 2015.
Available:http://www.esa.int/Our_Activities/Observing_the_Earth/Copernicus/Sentinel-2/Facts_and_figures
17. Shuttle Radar Topography Mission. Accessed: 17 November 2015.
Available: http://www2.jpl.nasa.gov/srtm/
18. Allen T, Wald D. On the use of high-resolution topographic data as a proxy for seismic site conditions (VS30). Bulletin of the Seismological Society of America. 2009;99(2A):935-943.
DOI: 10.1785/0120080255.
(Accessed: 2 January 2012)
Available:http://earthquake.usgs.gov/hazards/apps/vs30/allen_wald_2009_toposlope.pdf
19. Allen TI, Wald DJ, Hotovec AJ, Lin K, Earle PS, Marano KD. An Atlas of ShakeMaps for selected global earthquakes: U.S. Geological Survey Open-File Report, 2008-1236. 2012;34.
(Accessed: 11 October 2012)
Available:http://pubs.usgs.gov/of/2008/1236/downloads/OF08-1236_508.pdf
20. USA.com, South Dakota Natural Disasters and Weather Extremes.
(Accessed: 22 October 2015)
Available:http://www.usa.com/south-dakota-state-natural-disasters-extremes.htm
21. USGS Earthquake Hazards Program. Search Earthquake Archives.
(Accessed: 08 November 2015)
Available:http://earthquake.usgs.gov/earthquakes/search/

22. South Dakota Geological Survey. Accessed: 16 November 2015.
Available:http://www.sdgs.usd.edu/publications/maps/earthquakes/earthquakes.htm
23. Roggenthen WM. Earthquake potential in South Dakota, Proc. S.D. Acad. Sci. 1990; 69:143.2.
24. Schneider G. Erdbeben. Eine einführung für geowissenschaftler und bauingenieure. Spektrum Akademischer Verlag, Elsevier München. 2004;246.
25. Hannich D, Hötzl H, Cudmani R. Einfluss des grundwassers auf die schadenswirkung von erdbeben – ein Überblick. Grundwasser. 2006;11(4):286-294.
26. Theilen-Willige B, Aher SP, Gawali PB, Venkata LB. Seismic hazard analysis along Koyna Dam Area, Western Maharashtra, India: A contribution of remote sensing and GIS. Geosciences 2016;6:20.
DOI: 10.3390/geosciences6020020,
Available:http://www.mdpi.com/2076-3263/6/2/20
27. Carter JM, Williamson JE, Teller RW. The 1972 Black Hills-Rapid City Flood Revisited. U.S. Geological Survey, USGS Fact Sheet FS-037-02.
(Accessed: 15 November 2015)
Available:http://pubs.usgs.gov/fs/fs-037-02/
28. Theilen-Willige B, Charif A, Chaïbi M, Ait Malek H. Flash floods in the Guelmim area / SW-Morocco - Use of Remote Sensing and GIS-Tools for the Detection of Flooding Prone Areas. Geosciences. 2015; 5(2):203-221.
DOI: 10.3390/geosciences5020203,
Available:http://www.mdpi.com/2076-3263/5/2/203
29. South Dakota Department of Environment & Natural Resources, Other South Dakota GIS Datasets.
Floodzones-FEMA.
(Accessed: 12.01.2016)
Available:http://arcgis.sd.gov/server/sdgis/Data.aspx
30. Epstein JB, Doctor DH. Evaporite Karst in the Black Hills, South Dakota and Wyoming, and the Oil Play in the Williston Basin, North Dakota and Montana. 13th Sinkhole Conference, NCKRI SYMPOSIUM. 2012;2:161-176.
(Accessed 11 May 2012)
Available:http://www.infocastinc.com/downloads_pdf/bakken11_pre.pdf
http://scholarcommons.usf.edu/cgi/viewcontent.cgi?article=1124&context=sinkhole_2013
31. Epstein JB. Hydrology, Hazards, and Geomorphic Development of Gypsum Karst in the Northern Black Hills, South Dakota and Wyoming. In Eve L. Kuniansky, editor, 2001, U.S. Geological Survey Karst Interest Group, Proceedings, Water-Resources Investigations Report. 2001;01-4011:30-37.
Available:http://water.usgs.gov/ogw/karst/kigconference/jbe_hydrologyhazards.htm
32. Epstein J. Gypsum Karst Collapse in the Black Hills, South Dakota, Wyoming, USA. Acta Carsologica. 2000;2(7):103-122.
33. Stetler LD, Davis AD. Gypsum and Carbonate Karst along the I-90 Development Corridor, Black Hills, South Dakota.
Available:http://pubs.usgs.gov/sir/2005/5160/PDF/Part3_1.pdf
34. Theilen-Willige B, Malek HA, Charif A, El Bchari F, Chaïbi M. Remote sensing and GIS contribution to the investigation of Karst landscapes in NW-Morocco. Geosciences. 2014;4:50-72.
DOI: 10.3390/geosciences4020050
Accessed: 01 July 2014.
Available:http://www.mdpi.com/2076-3263/4/2/50

APPENDIX

GIS- Shapefile Data:

USGS, Mineral Resources On-Line Spatial Data:

http://mrdata.usgs.gov/geology/state/state.php?state=SD
http://mrdata.usgs.gov/geology/state/state.php?state=WY
The Bureau of Information and Telecommunications (BIT), State of South Dakota, GIS-South Dakota, http://arcgis.sd.gov/server/sdgis/Data.aspx
USGS, The National Map, http://viewer.nationalmap.gov/theme/elevation/#
http://viewer.nationalmap.gov/basic/#startUp
USGS. http://www.usa.com/south-dakota-state-natural-disasters-extremes.htm
USGS. Vs30 –data: http://earthquake.usgs.gov/hazards/apps/vs30/custom.php

Peer-review history:
The peer review history for this paper can be accessed here:
http://sciencedomain.org/review-history/14394